

## Multiple Sclerosis Lesions: Characterization with Texture Analysis technique Using MR Imaging

\*Simaa Khayal, Suhaib Alameen, Mohamed E. M. Gar-Elnabi

College of Medical Radiologic Science, Sudan University of Science and Technology, Khartoum, Sudan

Corresponding Author: Simaa Khayal

---

**Abstract:** This study concern to classify of brain tissues to multiple Sclerosis, White and Grey matter and CSF in MR Images, and the features of the classified regions of the whole images as raw data were classified furthers using linear discriminate analysis. The classification processes were carried out using Interactive Data Language (IDL) program as platform for the generated codes the result of the classification showed that the Multiple Sclerosis areas were classified well from the rest of the tissues although it has characteristics mostly similar to surrounding tissues. The step wise function selected three features mean, energy and entropy which gives a classification accuracy 94.2% for MS the sensitivity was 90.9% and the Specificity was 94.7%. While T2 weighted image gives a classification accuracy 93,7 % which is slightly less than T 1 weighted image for MS, the sensitivity was 86% which is obviously better in T1 weighted images than T2 and the specificity was 95,6%. And the flair gives a classification accuracy 93,3% which is slightly less than T 1 & T2 weighted images for MS, the sensitivity was 89% which is obviously better than T2 weighted images and the specificity was 94,7%. These relationships are stored in a Texture Dictionary that can be later used to automatically annotate new CT images with the appropriate pancreas area names.

**Keywords:** MRI, IDL, Multiple Sclerosis, Brain Tissue

---

Date of Submission: 09-04-2018

Date of acceptance: 23-04-2018

---

### I. Introduction

Magnetic resonance (MR) imaging is the most powerful preclinical tool for diagnosing and monitoring over time patients with multiple sclerosis (MS). MR imaging is particularly sensitive to the white matter (WM) disease associated with MS because WM changes affect many measurable MR imaging parameters, including proton density [1,2], water diffusion [3], T1 and T2 relaxation times [4–6], and cross relaxation [7,8]. Changes in these parameters are interpreted as indicators of myelin and axon loss, which may follow the initial inflammatory process in MS-induced WM lesions.

MS lesions exhibit hypersignals in T2 and hypo-signals in T1, with respect to normal white matter intensities. Typically, lesions appear smaller in T1 than T2, reflecting their complex internal structure. T1 lesion load has already been successfully correlated with the Expanded Disability Status Scale (EDSS) using large sets of patients, while there is little evidence of the clinical relevance of T2 lesion load [9]. In any case, an automatic segmentation system that generates different quantifiers is useful for diagnosis and clinical trials [10].

Conventional magnetic resonance imaging (MRI) techniques, such as T2-weighted (T2-w) and gadolinium enhanced T1-weighted (T1-w) sequences, are highly sensitive in detecting MS plaques and can provide quantitative assessment of inflammatory activity and lesion load. Although useful in the diagnosis and management of MS, conventional imaging has several limitations. Lesions are non-specific, indicating areas of inflammation, demyelination, ischemia, edema, cell loss, gliosis MRI-derived metrics have become the most important paraclinical tool for diagnosing MS, for understanding the natural history of the disease, and for monitoring the efficacy of experimental treatments [11].

Multiple sclerosis (MS) is a chronic inflammatory and neurodegenerative disease of the central nervous system characterized by inflammation, demyelination, oligodendrocyte loss, axonal and neuronal degeneration, gliosis, and remyelination [12,13]. and the most frequent, non-traumatic, neurological disease capable of causing disability in young adults. It is a chronic, persistent inflammatory-demyelinating, and degenerative disease of the central nervous system (CNS), characterized pathologically by areas of inflammation, demyelination, axonal loss, and gliosis scattered throughout the CNS, often causing motor, sensorial, vision, coordination, deambulation, and cognitive impairment [14].

In order to improve the accuracy of MRI and support early diagnosis of MS, it is crucial to quantify MRI abnormalities and apply image analysis techniques to MRI to capture diagnostically significant image features [15,16]. Among various image analysis techniques, texture analysis is useful especially in detecting subtle tissue changes and it has the potential to support early diagnosis of MS. In neuroimaging, texture analysis

has been used to detect lesions and abnormalities for quantifying contralateral differences in epilepsy [17] and hippocampal sclerosis [18], aiding the automatic delineation of cerebellar volumes [19], characterizing spinal cord pathology in MS [20] and following up therapeutic response for MS patients [21].

Several studies have investigated various MRI characteristics of MS patients. These studies have revealed tissue alterations, such as changes in both normal appearing brain tissue and lesions, in magnetization transfer ratio (MTR) [22,23]. In addition, abnormal brain iron deposits in the putamen and thalamus have been measured as T2 decrease [24-28] or phase development [29,30].

**Texture analysis Technique: First-Order Statistical:**

First-order texture analysis measure use the image histogram, or pixel occurrence probability, to calculate texture. The main advantage of this approach is its simplicity through the use of standard descriptors (e.g. mean and variance) to characterize the data (Press, 1998). However, the power of the approach for discriminating between unique textures is limited in certain applications because the method does not consider the spatial relationship, and correlation, between pixels. For any surface, or image, grey-levels are in the range  $0 \leq i \leq N_g - 1$ , where  $N_g$  is the total number of distinct grey-levels. If  $N(i)$  is the number of pixels with intensity  $i$  and  $M$  is the total number of pixels in an image, it follows that the histogram, or pixel occurrence probability, is given by,

$$P(i) = \frac{N(i)}{M}$$

In general, seven features commonly used to describe the properties of the image histogram, and therefore image texture, are computed. These are: mean; variance; coarseness; skewness; kurtosis; energy; and entropy. These textural features include First order statistics; (coefficient of variation, standard deviation, variance, signal, energy, and entropy). Images were classified the data concerning the brain tissues (Multiple Sclerosis, CSF, Bone, white and gray matter) and data entered to SPSS to generate a classification score using stepwise linear discriminate analysis; to select the most discriminate features that can be used in the classification of brain tissues in MR images.

**II. Methodology**

**Patients:** The sample of this study consists of 100 patients 62 female and 38 male, and the age ranged from 55 years to 80 years old were the mean of ages was 67.5 years.

**MRI Data acquisition:** The brain MRI protocol includes 3D T1-weighted, 3D T2-FLAIR, 3D T2-weighted, post-single-dose gadolinium-enhanced T1-weighted sequences images of the 100 patients were acquired from a 1.5-T MR scanner; GE at Modern Medical Center (Khartoum) using a turbo spin echo sequence [TR=5500 ms, TE=94 ms, number of excitation (NEX)=3, echo train length=11, matrix=256\*224, field of view (FOV)=240\*210 mm, slice thickness=4 mm and interslice gap=0.4 mm]. 100 regions of interests (ROIs) were chosen from MR images of MS patients for MS lesions and WM, GM, CSF and Bone respectively.

**III. Results**

The classification showed that the brain areas were classified well using T1 from the rest of the tissues although it has characteristics mostly similar to surrounding tissue.

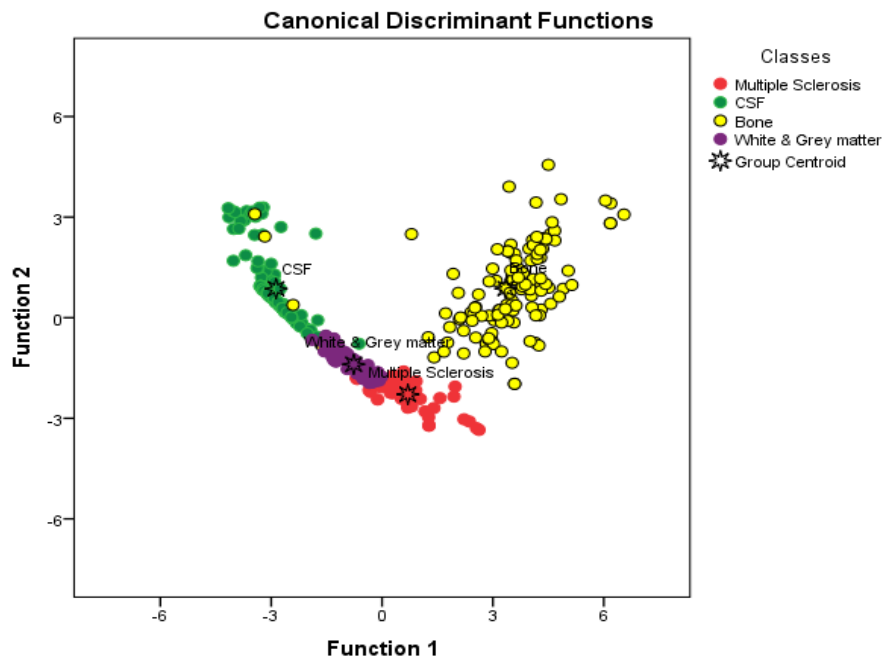


**Fig 1.** Scatter plot generated using discriminant analysis function for four classes represents: Multiple Sclerosis, CSF, White & Gray matter and bone.

**Table 1.** classification score matrix generated by linear discriminate analysis for the scatter plot using T1 shown in Fig 1. with classification accuracy of 94.2%

Original	Predicted Group Membership				Total
	Multiple Sclerosis	CSF	Bone	White & Grey matter	
Multiple Sclerosis	<u>90.9</u>	0.0	0.0	9.1	100.0%
CSF	0.0	<u>98.5</u>	0.0	1.5	100.0%
Bone	5.8	2.5	<u>90.0</u>	1.7	100.0%
White & Grey matter	4.3	0.0	0.0	<u>95.7</u>	100.0%

Sensitivity = 90.9%, Specificity = 94.7%, Accuracy = 94.2%

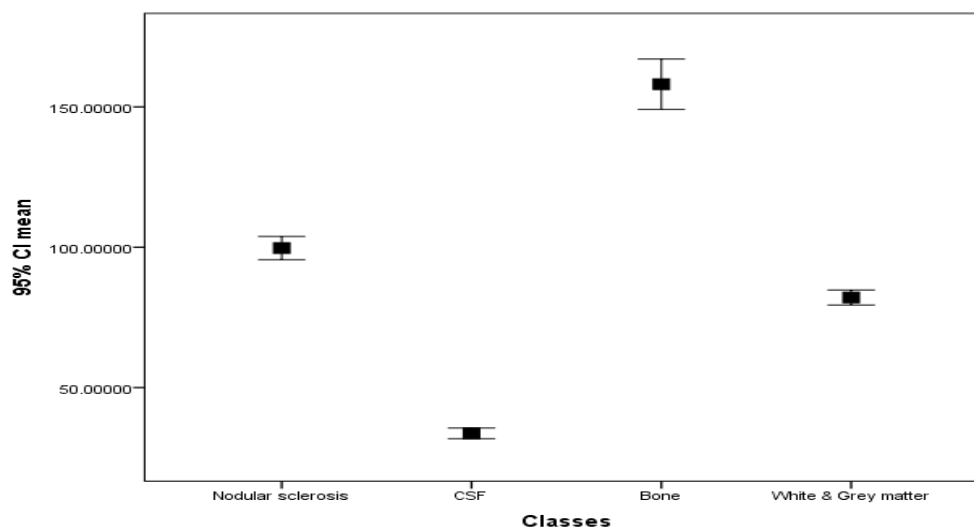


**Fig 2.** error bar plot for the mean textural features discriminate between the MS, CSF, Bone and White & Gray matter clearly.

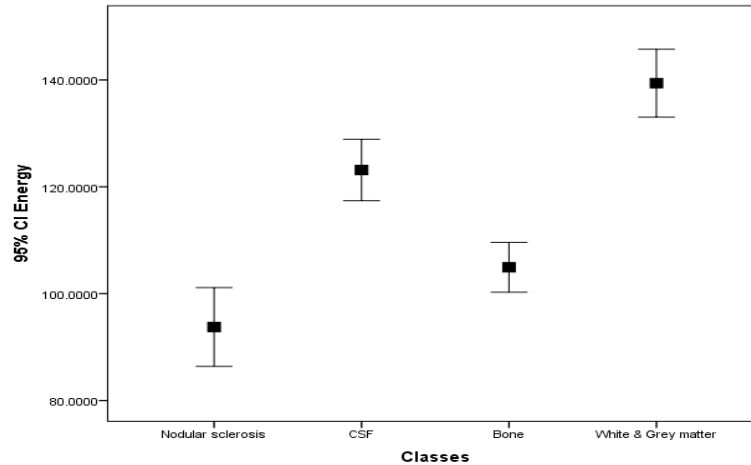


**Fig 3.** Error bar plot for the energy textural features that discriminate between the MS, CSF, Bone and White & Gray matter clearly.

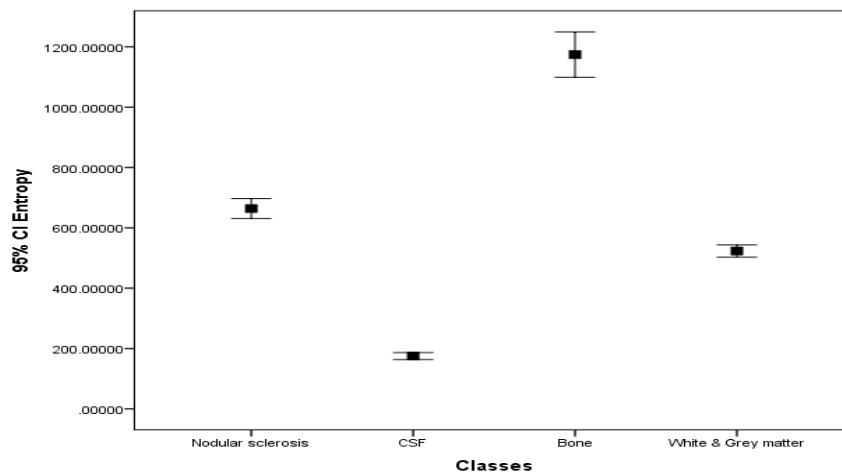


**Fig 4.** Error bar plot for the entropy textural features that discriminate between the MS, CSF, Bone and White & Gray matter clearly

The classification showed that the brain areas were classified well using T2 from the rest of the tissues although it has characteristics mostly similar to surrounding tissue.

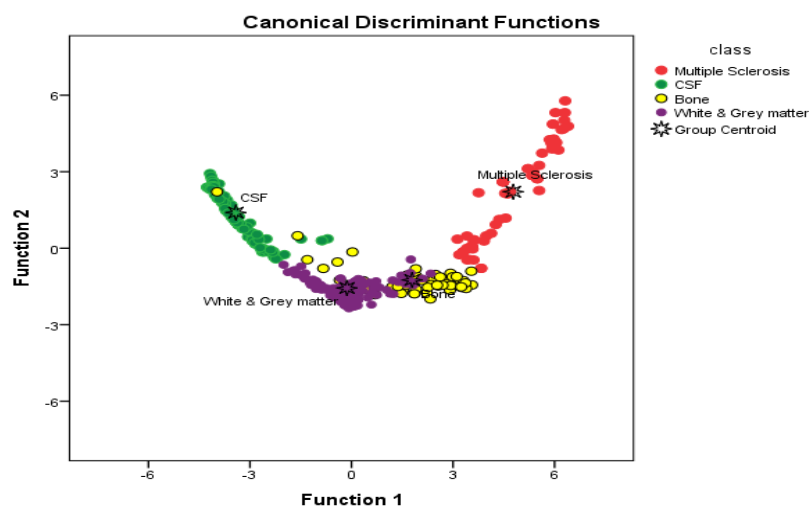


**Fig 5.** Scatter plot generated using discriminant analysis function for four classes represents: Multiple Sclerosis, CSF, White & Gray matter and bone.

**Table 2.** classification score matrix generated by linear discriminate analysis for the scatter plot using T2 shown in Fig5. with classification accuracy of 93.2%

Original	Predicted Group Membership				Total
	Multiple Sclerosis	CSF	Bone	White & Grey matter	
Multiple Sclerosis	<b>86.0</b>	0.0	14.0	0.0	100.0
CSF	0.0	<b>97.1</b>	2.9	0.0	100.0
Bone	0.0	3.4	<b>91.4</b>	5.2	100.0
White & Grey matter	0.0	0.0	1.6	<b>98.4</b>	100.0

Sensitivity = 86%, Specificity = 95.6%, Accuracy = 93.2%

Nodular sclerosis =  $(2.1 \times \text{mean}) + (0.019 \times \text{energy}) + (-0.207 \times \text{entropy}) - 50.6$

CSF =  $(1.329 \times \text{mean}) + (.054 \times \text{energy}) + (-0.166 \times \text{entropy}) - 9.1$

Bone =  $(3.2 \times \text{mean}) + (-.027 \times \text{energy}) + (-.375 \times \text{entropy}) - 37.18$

White and Grey matter =  $(3.189 \times \text{mean}) + (.019 \times \text{energy}) + (-.383 \times \text{entropy}) - 31.43$

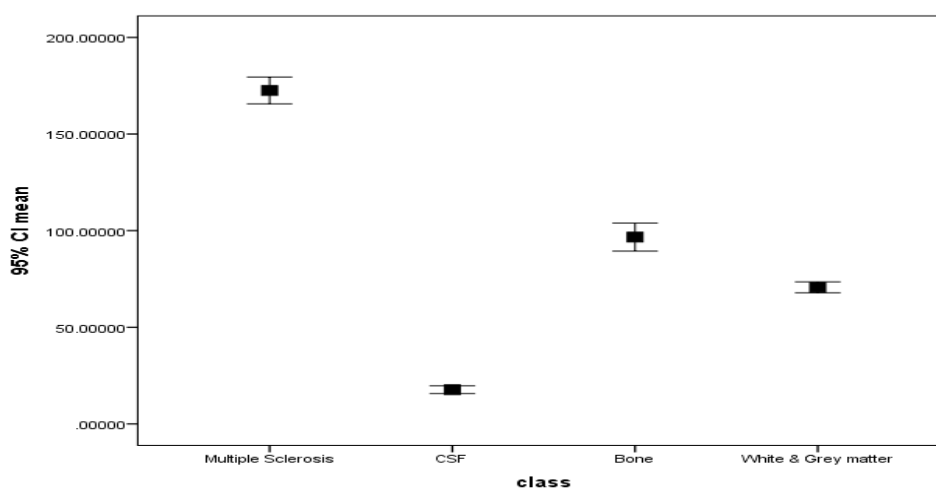


**Fig 6.**error bar plot for the mean textural features discriminate between the MS,CSF ,BONE and White &Gray matter clearly axial T2 Weighted image

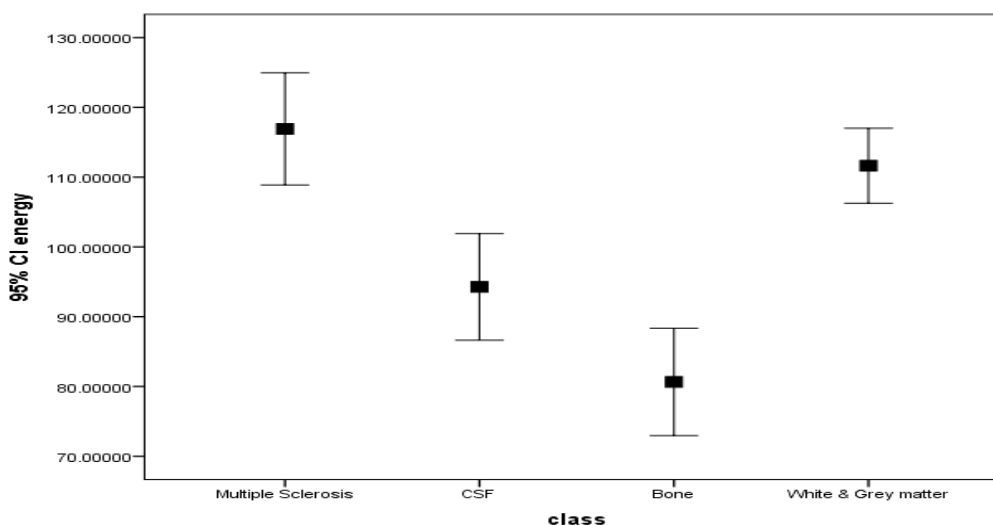


**Fig 7.**error bar plot for the energy textural features discriminate between the MS,CSF ,BONE and White &Gray matter clearly in axial T2 Weighted Images

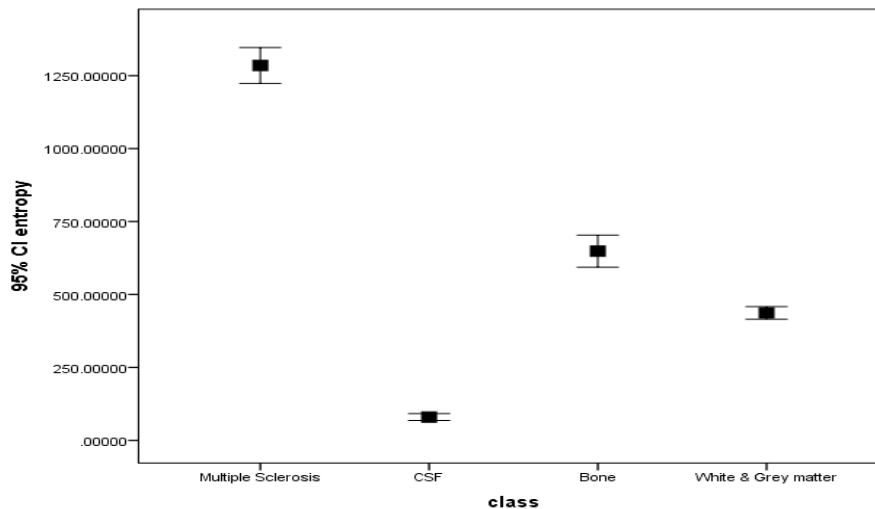


**Fig 8.** error bar plot for the entropy textural features that discriminate between the MS,CSF ,Bone and White & Gray matter clearly T2 weighted image.

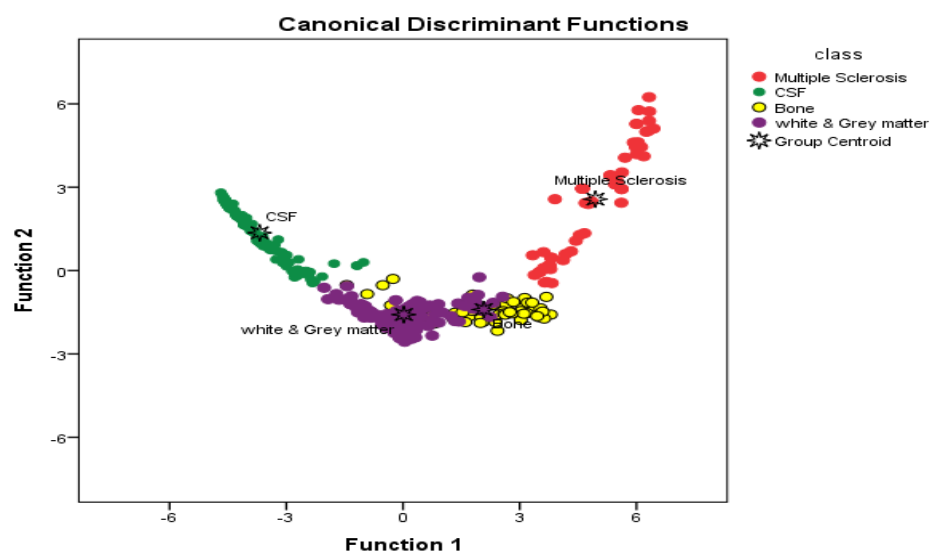


**Fig9.** Scatter plot generated using discriminant analysis function for four classes represents:Multiple Sclerosis, CSF, White & Gray matter and bone.

**Table3.** classification score matrix generated by linear discriminate analysis for the scatter plot using flairshown in Fig 9. with classification accuracy of 93.3%

Original	Predicted Group Membership				Total
	Multiple Sclerosis	CSF	Bone	white & Grey matter	
Multiple Sclerosis	<b>89.1</b>	0.0	10.9	0.0	100.0
CSF	0.0	<b>96.2</b>	2.8	.9	100.0
Bone	0.0	0.0	<b>91.1</b>	8.9	100.0
white & Grey matter	0.0	0.0	3.1	<b>96.9</b>	100.0

Sensitivity = 89.1%, Specificity =94.7%, Accuracy = 93.3%

Nodular sclerosis =  $(2.42 \times \text{mean}) + (0.023 \times \text{energy}) + (-0.242 \times \text{entropy}) - 56.6$

CSF =  $(1.45 \times \text{mean}) + (.051 \times \text{energy}) + (-0.179 \times \text{entropy}) - 9.53$

Bone =  $(3.73 \times \text{mean}) + (-.031 \times \text{energy}) + (-.435 \times \text{entropy}) - 40.37$

White and Grey matter =  $(3.56 \times \text{mean}) + (.006 \times \text{energy}) + (-.426 \times \text{entropy}) - 34.76$

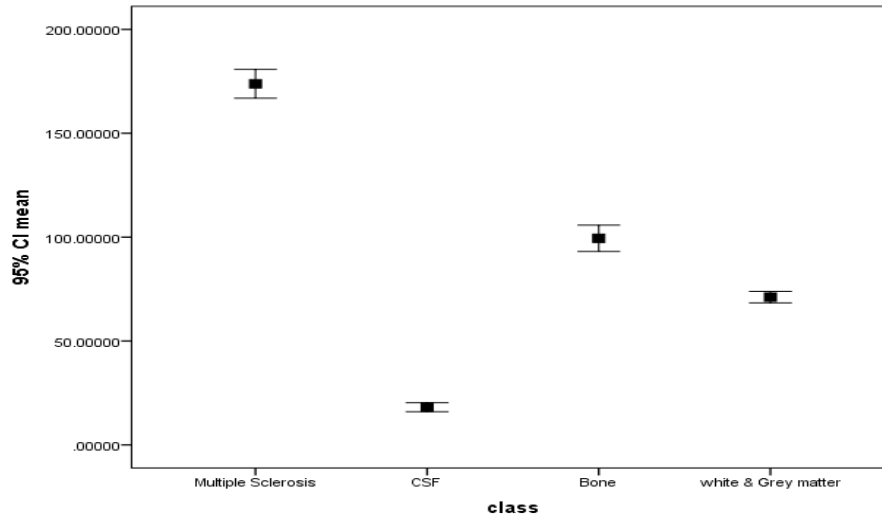


**Fig10.**error bar plot for the mean textural features discriminate between the MS,CSF ,BONE and White &Gray matter clearly in axial FLAIR Image

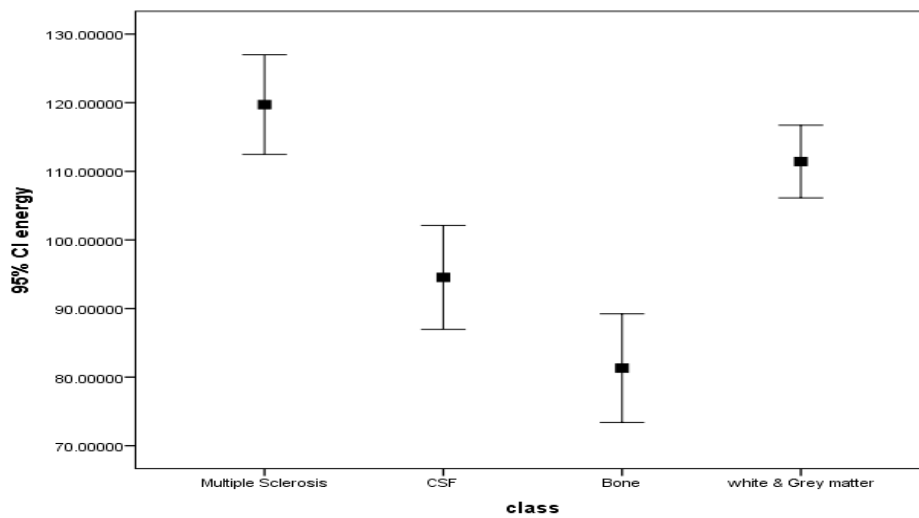


**Fig 11.**error bar plot for the energy textural features discriminate between the MS,CSF ,BONE and White &Gray matter clearly in axial FLAIR Image

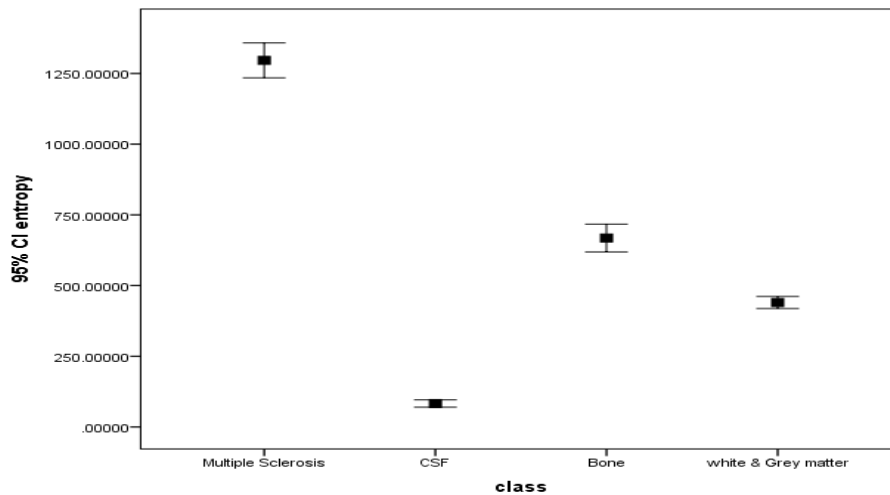


**Fig 12.**error bar plot for the entropy textural features discriminate between the MS,CSF ,BONE and White &Gray matter clearly in axial FLAIR Image

#### IV. Discussion

This study was intended to characterize multiple sclerosis in MR images using texture analysis first order statistic. In T1 images using discriminant analysis function where five features have been entered as input variable for four classes represents: Multiple Sclerosis, CSF, White & Gray matter and bone. The step wise function selected three features (mean, energy and entropy) which gives a classification accuracy 94.2% for MS the sensitivity was 90.9% and the Specificity was 94.7%.

These means multiple sclerosis can be identify with an excellent precision and meanly the miss classify region attributed to miss identification of region of interest. The mean feature mostly discriminates the CSF and Bone from MS and white matter & Gray matter clearly.

While T2 weighted image gives a classification accuracy 93,7 % which is slightly less than T 1 weighted image for MS, the sensitivity was 86% which is obviously better in T1 weighted images than T2 and the specificity was 95,6%. The mean feature mostly discriminates between the MS, bone and white matter & gray matter. The energy textural feature shows poor discrimination because the contrast in T2 weighted image was limited. Entropy feature discriminate between MS and CSF clearly better than T1 weighted image where MS reveals high randomness. The flair gives a classification accuracy 93,3% which is slightly less than T 1 & T2 weighted images for MS, the sensitivity was 89% which is obviously better than T2 weighted images and the specificity was 94,7%. In this study there were three features extracted from normal and abnormal (multiple sclerosis) brain MRI image T1, T2 and Flair. From these features, the three showed significant correlation with the predefined classes (multiple sclerosis, bone, CSF and white & grey matter) they include mean, entropy, energy, and variance. The classification maps as shown in Fig 1. were generated by using Euclidian distance, where the center of the classes chosen arbitrary from areas represented the classes of interest. In T1 images using magnetic resonance.

#### V. Conclusion

The classification of brain tissues to multiple Sclerosis, White and Grey matter and CSF in MR Images and the features of the classified regions of the whole images as raw data were classified further using linear discriminate analysis. The classification processes were carried out using Interactive Data Language (IDL) program as platform for the generated codes the result of the classification showed that the Multiple Sclerosis areas were classified well from the rest of the tissues although it has characteristics mostly similar to surrounding tissues. Using Linear discrimination analysis generated a classification function which can be used to classify other image into the mention classes as using the following multi regression equation; where the vote will be for the class with a higher classification score:

$$\text{Nodular sclerosis} = (3.73 \times \text{mean}) + (-0.054 \times \text{energy}) + (-0.44 \times \text{entropy}) - 38.93$$

$$\text{CSF} = (1.79 \times \text{mean}) + (.076 \times \text{energy}) + (-0.217 \times \text{entropy}) - 17.317$$

$$\text{Bone} = (2.96 \times \text{mean}) + (-.028 \times \text{energy}) + (-0.339 \times \text{entropy}) - 35.280$$

$$\text{White and Grey matter} = (3.16 \times \text{mean}) + (0.031 \times \text{energy}) + (-.375 \times \text{entropy}) - 35.03$$

#### References

- [1]. Gilmore CP, DeLuca GC, Bö L, et al. Spinal cord neuronal pathology in multiple sclerosis. *Brain Pathol* 2009; 19 (4): 642 – 649.
- [2]. Bagnato F, Yao B, Cantor F, et al. Multisequence-imaging protocols to detect cortical lesions of patients with multiple sclerosis: observations from a post-mortem 3 Tesla imaging study. *J Neurol Sci* 2009; 282 (1-2): 80 – 85.
- [3]. Goldberg-Zimring D, Mewes AU, Maddah M, Warfield SK. Diffusion tensor magnetic resonance imaging in multiple sclerosis. *J Neuroimaging* 2005; 15 (4, Suppl): 68S – 81S.
- [4]. Parry A, Clare S, Jenkinson M, Smith S, Palace J, Matthews PM. White matter and lesion T1 relaxation times increase in parallel and correlate with disability in multiple sclerosis. *J Neurol* 2002; 249 (9): 1279 – 1286.
- [5]. Bakshi R, Benedict RH, Bermel RA, et al. T2 hypointensity in the deep gray matter of patients with multiple sclerosis: a quantitative magnetic resonance imaging study. *Arch Neurol* 2002; 59 (1): 62 – 68.
- [6]. Laule C, Vavasour IM, Moore GR, et al. Water content and myelin water fraction in multiple sclerosis: a T2 relaxation study. *J Neurol* 2004; 251 (3): 284 – 293.
- [7]. Karampekios S, Papanikolaou N, Papadaki E, et al. Quantification of magnetization transfer rate and native T1 relaxation time of the brain: correlation with magnetization transfer ratio measurements in patients with multiple sclerosis. *Neuroradiology* 2005; 47 (3): 189 – 196.
- [8]. Chen JT, Kuhlmann T, Jansen GH, et al. Voxel-based analysis of the evolution of magnetization transfer ratio to quantify remyelination and demyelination with histopathological validation in a multiple sclerosis lesion. *Neuroimage* 2007; 36 (4): 1152 – 1158.
- [9]. A. Tourbah, "IRM et scl' erose en plaques," *Neurologies*, vol. 4, no. 33, pp. 270–274, 2001.
- [10]. J. Grimaud, Y.-M. Zhu, and M. Rombaut, "Mise au point : Les techniques d'analyse quantitative des IRM c' er'ebrales : application 'alasc' erose en plaque," *Revue Neurologique*, vol. 158, no. 3, pp. 381–389, 2002.
- [11]. van den Elskamp IJ, Boden B, Dattola V, Knol DL, Filippi M, Kappos L, Fazekas F, Wagner K, Pohl C, Sandbrink R, Polman CH, Uitdehaag BMJ, Barkhof F (2010) Cerebral atrophy as outcome measure in short-term phase 2 clinical trials in multiple sclerosis. *Neuroradiology* 52(10):875–881
- [12]. Keegan BM, Noseworthy JH. Multiple sclerosis. *Annu Rev Med* 2002; 53:285–302.

- [13]. Prineas JW, Kwon EE, Cho ES, et al. Immunopathology of secondary-progressive multiple sclerosis. *Ann Neurol* 2001;50:646–657.
- [14]. Compston A, Coles A (2006) Multiple sclerosis. *Lancet* 359(9313):1221–1231
- [15]. M. M. Galloway, “Texture analysis using gray level run lengths,” *Computer Graphics and Image Processing*, vol. 4, no. 2, pp. 172–179, 1975.
- [16]. H. Zhu, Y. Zhang, X. Wei, L. M. Metz, and J. R. Mitchell, “MR multi-spectral texture analysis using space-frequency information,” in *Proceedings of the International Conference on Mathematics and Engineering Techniques in Medicine and Biological Sciences (METMBS '04)*, pp. 173–179, June 2004.
- [17]. R. A. Brown and R. Frayne, “A comparison of texture quantification techniques based on the Fourier and S transforms,” *Medical Physics*, vol. 35, no. 11, pp. 4998–5008, 2008.
- [18]. S. G. Mallat, “A theory for multiresolution signal decomposition: the wavelet representation,” *IEEE Transactions on Pattern Analysis and Machine Intelligence*, vol. 11, no. 7, pp. 674–693, 1989.
- [19]. R. G. Stockwell, L. Mansinha, and R. P. Lowe, “Localization of the complex spectrum: the S transform,” *IEEE Transactions on Signal Processing*, vol. 44, no. 4, pp. 998–1001, 1996.
- [20]. Y. Zhou, *Boundary detection in petrographic images and applications of S-transformspace-wavenumber analysis to image processing for texture definition*, Ph.D. thesis, The University of Western Ontario, 2002.
- [21]. M. E. Mayerhoefer, P. Szomolanyi, D. Jirak, A. Materka, and S. Trattnig, “Effects of MRI acquisition parameter variations and protocol heterogeneity on the results of texture analysis and pattern discrimination: an application-oriented study,” *Medical Physics*, vol. 36, no. 4, pp. 1236–1243, 2009.
- [22]. Bellmann-Strobl, J., Stiepani, H., Wuerfel, J., et al.(2009) MR spectroscopy (MRS) and magnetisation transfer imaging (MTI), lesion load and clinical scores in early relapsing remitting multiple sclerosis: A combined cross-sectional and longitudinal study. *European Radiology*, 19, 2066-2074. doi:10.1007/s00330-009-1364-z
- [23]. Hayton, T., Furby, J., Smith, K.J., et al.(2009) Grey matter magnetization transfer ratio independently correlates with neurological deficit in secondary progressive multiple sclerosis. *Journal of Neurology*, 256, 427-435. doi:10.1007/s00415-009-0110-4
- [24]. Drayer, B., Burger, P., Hurwitz, B., et al.(1987) Reduced signal intensity on MR images of thalamus and putamen in multiple sclerosis: Increased iron content? *American Journal of Roentgenology*, 149, 357-363. doi:10.2214/ajr.149.2.357
- [25]. Brass, S.D., Chen, N.K., Mulkern, R.V., et al.(2006) Magnetic resonance imaging of iron deposition in neurological disorders. *Topics in Magnetic Resonance Imaging*, 17, 31-40.
- [26]. Khalil, M., Enzinger, C., Langkammer, C., et al.(2009) Quantitative assessment of brain iron by R(2)\* relaxometry in patients with clinically isolated syndrome and relapsing-remitting multiple sclerosis. *Multiple Sclerosis*, 15, 1048-1054. doi:10.1177/1352458509106609
- [27]. Neema, M., Arora, A., Healy, B.C., et al.(2009) Deep gray matter involvement on brain MRI scans is associated with clinical progression in multiple sclerosis. *Journal of Neuroimaging*, 19, 3-8. doi:10.1111/j.1552-6569.2008.00296.x
- [28]. Ceccarelli, A., Rocca, M.A., Neema, M., et al.(2010) Deep gray matter T2 hypointensity is present in patients with clinically isolated syndromes suggestive of multiple sclerosis. *Multiple Sclerosis*, 16, 39-44. doi:10.1177/1352458509350310
- [29]. Haacke, E.M., Makki, M., Ge, Y., et al.(2009) Characterizing iron deposition in multiple sclerosis lesions using susceptibility weighted imaging. *Journal of Magnetic Resonance Imaging*, 29, 537-544. doi:10.1002/jmri.21676
- [30]. Mittal, S., Wu, Z., Neelavalli, J., et al.(2009) Susceptibility-weighted imaging: Technical aspects and clinical applications, part 2. *American Journal of Neuroradiology*, 30, 232-252. doi:10.3174/ajnr.A1461

Simaa Khayal "Multiple Sclerosis Lesions: Characterization with Texture Analysis technique Using MR Imaging" *IOSR Journal of Applied Physics (IOSR-JAP)* , vol. 10, no. 2, 2018, pp. 18-26.